Indian Journal of Biochemistry & Biophysics
Vol. 63, October 2026, pp. 1158-1168
DOI: 10.56042/ijbb.v63i10.24642

In silico study on assembly of Dengue virus capsid protein with core histone proteins

Dwaipayan Chaudhuri and Kalyan Giri*

Department of Life Sciences, Presidency University, Kolkata-700 073, West Bengal, India

Received 08 October 2025; *revised 05 July 2026*

The Dengue virus (DENV), a member of the Flaviviridae family, is a rapidly spreading pathogen that infects millions of people every year causing severe illness. The capsid (C) protein is in charge of assembling the viral RNA into a nucleocapsid. A significant amount of capsid protein relocates to the nucleus, although viral replication takes place in the cytoplasm. DENV C interacts with the four core histones according to earlier research. Therefore, DENV C functions to bind DNA and interfere with the assembly of nucleosomes through heterodimerization with core histones. Using coarse-grained *in silico* assembly simulations and comprehensive MD simulations to examine the interaction between the proteins, we have elucidated on the pattern of interaction between the DENV C protein and the histone proteins. Here it was seen that the interaction strength of DENV C and histones is as follows: H3> H2B> H2A> H4 with all interactions being highly stable. Our study also identifies critical residues (majorly hydrophobic residues in the hydrophobic pocket and H4 helix) in the DENV C protein responsible for these interactions. This study opens up new possibilities for antiviral drug design by advancing our understanding of the molecular interactions between viral proteins and host cell machinery.

Keywords: Capsid protein, Coarse grained assembly simulation, Contact analysis, Histones

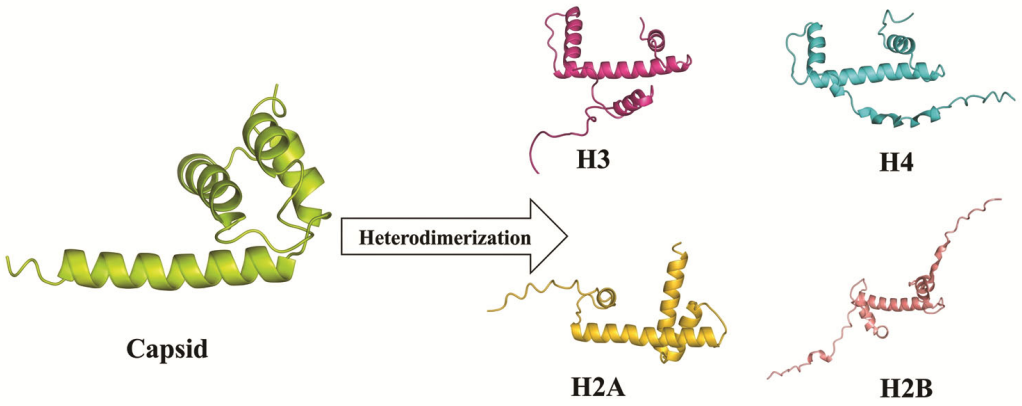
Dengue virus (DENV) belongs to the family *Flaviviridae* and is a globally emerging pathogen that leads to serious human disease culminating in millions of infections every year throughout the globe specifically in tropical and sub-tropical countries. The flaviviral RNA genome encodes a single precursor polyprotein which is cleaved co- and post-translationally into three structural and seven non-structural (NS) proteins by viral and cellular proteases[1]. Mature DENV capsid protein (C) is a small, highly basic 12-kDa protein and an essential factor during virion assembly. Flavivirus capsid (C) is a structural protein responsible for gathering the viral genomic positive sense single stranded RNA and packaging it to form a nucleocapsid thus forming the core of a mature virus particle. DENV C is involved in the proper encapsidation of the RNA genome, resulting in a spherical nucleocapsid with a single copy of the ssRNA molecule[2]. Flaviviral replication is known to occur in the cytoplasm along with the perinuclear region of the ER yet a large portion of capsid protein localizes to the nucleus during infection[3,4].

*Correspondence:
Email: kalyan.dbs@presiuniv.ac.in
Suppl. data available on respective page of NOPR

DENV C was detected to be bound with recombinant histones in solution and colocalized with histones in the nucleus and cytoplasm of liver cells during DENV infection. Earlier researches suggest that the DENV C protein can mimic the structure of the core histone as well in turn forming heterodimers with core histones, binding DNA, ultimately disrupting nucleosome formation. The interactions of C and histones thus, add an interesting new role for the presence of C in the nucleus during DENV infection[5].

Histones are known to form dimers through interactions between hydrophobic amino acids located in their second and third alpha helices[6]. DENV C is also an alpha-helical protein with the ability to self-dimerize and contains a large number of hydrophobic residues in its second alpha helix[7]. It has been seen that this capsid-histone interaction does not affect the histone-DNA interaction, in fact capsid protein has also been shown to interact with the DNA in absence of histone proteins as well. But, it has been observed that this interaction between the DENV C protein and the histone proteins prevents assembly of the nucleosome and histone dimers in the infected cell.

Here we have tried to shed light on the binding mode between the DENV C and the core histone



Graphical abstract

proteins leading to their heterodimerization. *In silico* assembly simulations of the viral C protein and the core histone proteins were performed such that no long range interactions take place between the capsid protein and the histone proteins prior to the simulation taking place. The importance of the various capsid protein residues in complex formation have also been discussed in great detail in this study. This study thus sheds light on the mode of interaction between the DENV C and the histone proteins helping to characterize the intricacies of this step of the viral life cycle inside the host cell.

Materials and Methods

Coarse-grained assembly of capsid protein with histone proteins

The structure of the DENV C protein was taken from 1r6r.pdb following loop remodeling since the first twenty amino acids from the N-terminal end constituting the disordered segment of the capsid protein is absent in the structure. The structure of the histone proteins was all taken from 4z5t.pdb. The capsid protein along with each of the four histone proteins that comprise the core histone octamer were taken together to form four complexes each with one copy of the capsid protein and one copy of histone protein. The coarse-grained model was generated through the CHARMM-GUI Martini Maker tool, which applied the MARTINI force field to map the protein and water molecules[8]. The resulting coarse-grained protein system was placed in a water box. The system solvation was performed with the MARTINI water model, and additional counter-ions were added to neutralize the solvated system. The solvated system underwent two levels of steepest descent minimization using GROMACS 2021.5 where each level of minimization was performed for 3000 steps each to remove any steric clashes or unrealistic geometry arising from the coarse-graining process[9]. The convergence criterion was set to a maximum force of 1000 kJ/mol/nm. This step was performed to ensure that the system reaches a stable configuration before the production runs are initiated. The energy minimized protein-protein complex system was equilibrated for 1000 ps under NPT (constant number of particles, pressure, and temperature) conditions where the heavy atoms of the protein were position-restrained to ensure that the initial coarse-grained structure was not disturbed during the thermalization process. The temperature was set to 310 K using the V-rescale thermostat, and the pressure was maintained at 1 bar using the Parrinello-Rahman barostat[10,11]. Production molecular dynamics (MD) simulations were performed to study the dynamics of the protein assembly process in its coarse-grained form. The production run was carried out for a total duration of 1 μs under NPT conditions at 310 K and 1 bar. The V-rescale thermostat and Parrinello-Rahman barostat were used to maintain the temperature and pressure, respectively. A time step of 20 fs during the production run, a value suitable for the coarse-grained model, which allows for longer time steps due to the reduced degrees of freedom. To enhance the sampling of conformational space, long-range electrostatic interactions were calculated using the reaction-field method and a cut-off of 1.2 nm[12]. Van der Waals interactions were computed using a cut-off of 1.2 nm as well. The periodic boundary conditions were applied to the simulation box to simulate an infinite system and minimize finite size effects. Clustering analysis of the generated trajectory was performed making use of in-built gromacs commands and

linkage method of clustering. The process of assembly was also analysed by studying the evolution of distance between the center of masses of the two proteins in consideration in the respective systems as the assembly process proceeds through a decrease in the distance between the center of masses. Capsid-histone protein complex structure which serves as the central structure of the densest cluster was taken for further analysis.

MD simulation and post simulation analysis of capsid-histone protein-protein complex

The capsid-histone protein complex structure extracted from each of the 1μs coarse-grained MD simulation trajectories was first converted to all-atom configuration making use of the all atom converter module present in CHARMM-GUI web server[13]. The all atom systems were prepared using CHARMM-GUI web server using the TIP3P water model in a cubic simulation box using the CHARMM36 forcefield. A distance of 1 nm between the protein and simulation box boundary was selected during system preparation. Additionally, counter-ions (Na^+ and Cl^-) were added such as to neutralize the system and simulate a physiological concentration of 0.15 M NaCl. An energy minimization was performed using the steepest descent algorithm to remove any steric clashes and relax the system before the equilibration and production run. The protein-protein complex system was minimized until the maximum force on any atom was reduced to below 1000 kJ/mol/nm to get rid of any high-energy configurations. The energy minimized system was equilibrated in NPT condition with 1 bar pressure and 310 K temperature for 500 ps using the Parrinello-Rahman barostat to adjust the system's pressure and maintain its density. The V-rescale thermostat was employed for temperature regulation and maintenance. The production molecular dynamics (MD) simulation was carried out thrice for each system in the NPT ensemble at a constant temperature of 310 K and pressure of 1 bar for a total simulation time of 500 ns each. The simulation was performed using a time step of 2 fs. The LINCS algorithm was used to constrain bond lengths and long range electrostatic interactions were computed using the PME (Particle Mesh Ewald) method and a cut-off of 1.2 nm[14]. Van der Waals interactions were computed using a cut-off of 1.2 nm as well. GROMACS in-built commands were used for post simulation analysis purpose in order to characterize the nature and specificity of interaction between DENV C protein and the histone proteins. The g_mmpbsa module was used for binding energy calculation[15]. Contact analysis of the capsid-histone complexes were performed for the last 50 ns taken from all the three 500 ns MD simulation trajectories using the get Contacts module.

Results and Discussion

Coarse grained assembly of the Capsid-histone complexes

The DENV C protein and the histone proteins were initially placed at a minimum separation of 5 nm from each other in a random orientation. A higher distance between the two proteins was selected so as to eliminate any possibility of long range interactions taking place between them. Through the course of the unrestrained coarse grained MD simulation it was observed that following an initial extended equilibration period, the capsid protein came in close proximity of the histone proteins in case of all the four systems under consideration in this study. This process of moving of the capsid and histone protein in close proximity of each other in order to form a stable complex could be easily visualized from the decreasing trend of the distance between the center of masses of the two proteins through the course of the 1μs coarse grained MD simulation performed here (Fig. 1A). It can be seen that except for the complex between C and histone H4, the other heterodimeric complexes were formed within the first 200 ns of the MD simulation runs. In case of the heterodimeric complex between capsid protein and the histone H4, stable complex was formed for the last 200 ns of the MD simulation run. In this last 200 ns of the 1μs MD simulation trajectory all the complexes formed were found to be highly stable in nature. This highly stable nature of the formed complexes could be seen from the plateau formation of the RMSD evolution of the protein complex through the course of the MD simulation trajectory (Fig. 1B). RMSD trajectory also follows similar trends like the distance between the center of masses of the two proteins under consideration in this study. This provides further evidence on the highly stable nature of the complexes generated through the course of the MD simulation run. In case of all the histone proteins except H4, a RMSD plateau could be seen to be achieved within the first 175-200 ns of MD simulation run, while a plateau can be seen to be attained for the last 300 ns approximately in case of the complex between DENV C protein and histone H4 proteins.

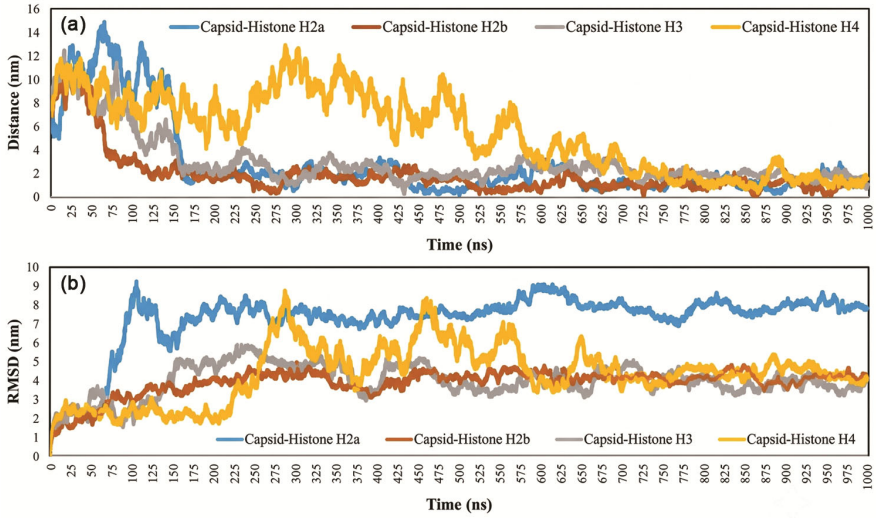


Fig. 1 — Coarse grained assembly of C protein and histone proteins. A. Distance between center of mass of C protein and histone proteins through the course of 1µs coarse grained MD simulation. B. RMSD evolution of C protein and histone proteins through the course of 1µs coarse grained MD simulation

MD simulation and post simulation analysis of capsid-histone complexes

The structures of the capsid-histone protein complexes were obtained following clustering analysis of the 1µs coarse grained assembly MD simulation trajectories of the capsid and histone protein systems. Through the course of the MD simulations conducted, structural equilibration and stabilization of the formed complexes was observed. Clustering was performed on the 500 ns MD simulation trajectories as well following catenation of the triplicate MD simulation trajectories, ultimately leading to the analysis being conducted on a simulation length of 1.5 µs in case of every single capsid and histone protein complex i.e. capsid protein in complex with H2A histone, H2B histone, H3 histone and H4 histone individually. In each case, formation of three prominent clusters was observed in the entire 1.5 µs MD simulation trajectory. Further analysis of the frames encompassing the three dominant clusters point to the convergence being reached in each of the three independent replica MD simulations conducted. MM/GBSA binding energy calculation was performed on all the cluster representative structures obtained from the MD simulations conducted. All three representative structures in case of each of the systems were seen to be having similar binding energy magnitudes with each of the complexes being highly stable in nature as can be seen from the high negative magnitude of the binding energy values computed in this study (Fig. 2).

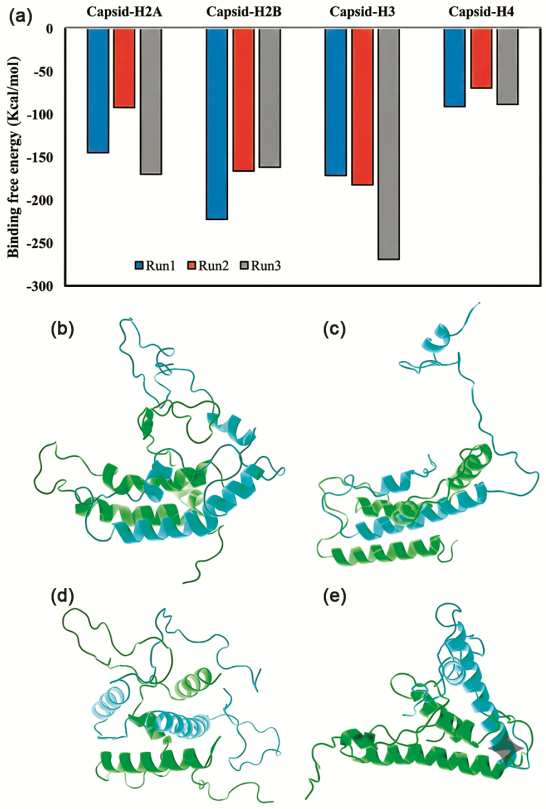
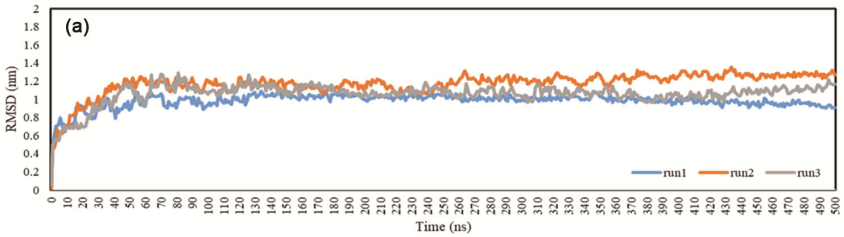


Fig. 2 — Capsid-histone complexes post MD simulation and clustering analysis. A. MM/GBSA Binding free energies of the capsid-histone protein complexes following 500 ns MD simulations in sets of three independent simulations. B. Capsid protein in complex with H2A histone. C. Capsid protein in complex with H2B histone. D. Capsid protein in complex with H3 histone. E. Capsid protein in complex with H4 histone. Capsid protein is coloured in green while the histone proteins are coloured in blue



(b)

Residue Mutation	PHE53	LEU95	LEU50	LEU81	LEU54	PRO12	LEU92
A	0.55	0.51	0.37	0.4	1.75	0.94	0.87
C	0.43	0.39	0.42	0.29	1.24	0.46	0.68
D	0.79	0.85	1.08	0.77	1.61	0.81	1.22
E	0.85	0.97	0.7	0.69	1.25	1.29	0.99
F	0	0.03	0.25	0.01	0.43	0.32	0.29
G	0.8	0.88	0.83	0.84	1.96	1.08	1.16
H	0.51	0.52	0.61	0.29	0.91	0.58	0.74
I	0.26	0.21	0	-0.03	0.61	0.37	0.2
K	0.64	0.72	0.65	0.58	1.13	1.12	0.71
L	0.28	0	0	0	0	0.49	0
M	0.29	0.2	0.15	0.19	0.58	0.7	0.37
N	0.79	0.57	0.76	0.73	1.19	0.57	0.95
P	0.82	1.11	0.84	0.92	1.54	0	1.28
Q	0.6	0.61	0.49	0.46	1.11	0.91	0.73
R	0.55	0.56	0.47	0.34	0.97	0.73	0.43
S	0.63	0.5	0.65	0.62	1.75	0.54	0.99
T	0.61	0.35	0.59	0.57	1.32	0.36	0.81
V	0.43	0.37	0.09	0.22	0.78	0.34	0.48
W	-0.11	0.42	0.33	-0.06	-0.07	0.25	0.26
Y	0.05	0.27	0.31	-0.09	0.24	0.38	0.51

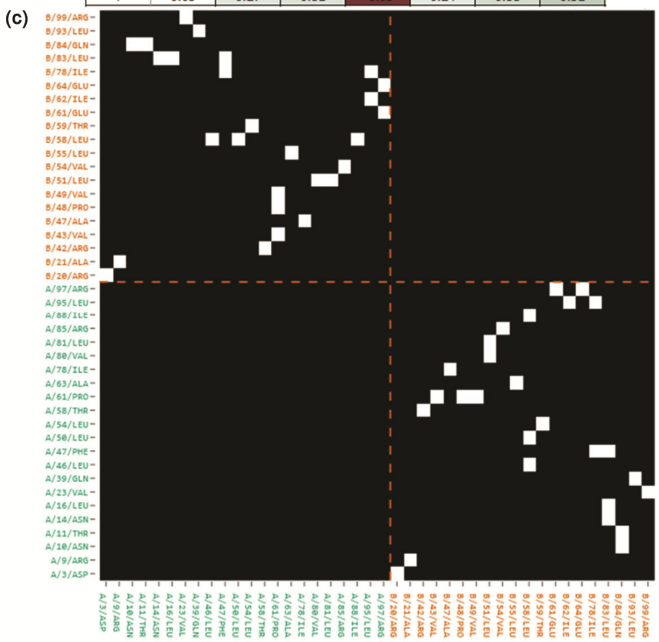


Fig. 3 — MD simulation and post simulation analysis of C protein in complex with H2A histone. A. RMSD evolution of the capsid-histone complex backbone atoms through the course of the three 500 ns MD simulation trajectories. B. Saturation mutagenesis analysis of the highest binding energy contributing residues of the capsid protein. C. Inter-chain contact map of Capsid protein in complex with Histone protein

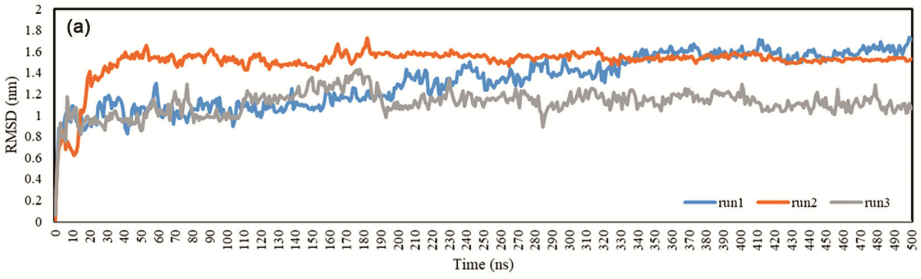
Capsid protein interaction with Histone H2A

RMSD trajectory of the protein backbone atoms for all the three 500 ns MD simulations conducted shows the formation of a RMSD plateau within the first 70 ns of the conducted MD simulations following which the statistical variance of the RMSD values become negligible in nature (Fig. 3A) indicative of the formation of structural convergence in this case. Residue wise binding energy analysis of the structurally stabilized complexes generated following clustering analysis show the predominant participation of the hydrophobic residues of both the capsid as well as the histone protein (Suppl. Table S1). Saturation mutagenesis of the

capsid protein residues showing highest contribution during complex formation shows most of the mutations to be destabilizing in nature (green colour in Fig. 3B) with few mutations having neutral and/or beneficial effect as well. This further stresses on the importance of these residues during interaction of the C and H2A protein. It can be seen that almost all the capsid protein residues that have been analyzed based on mutagenesis analysis are hydrophobic in nature with all the residues being part of the highly structured H2-H4 helical region of the capsid protein. Residues like Phe53, Leu50 and Leu54 show immense participation in the interaction between the capsid protein and H2A histone protein which are also important constituents of the capsid protein hydrophobic pocket. This high contribution of hydrophobic interactions indicates the importance of these interactions in histone octamer formation as well as capsid dimer formation[16]. Contact and long range interaction analysis as seen in (Fig. 3C) shows the active involvement of majorly hydrophobic interactions during the complex formation between the capsid protein and H2A histone. It can also be seen that a high number of residues belonging to the capsid protein hydrophobic pocket are involved in stable interaction with the H2A histone further emphasizing on the dominance of hydrophobic interactions in complex formation between the two proteins under consideration in this case. Contact analysis of the capsid-histone protein complex shows the active involvement of the hydrophobic pocket and H4 helix belonging to the DENV C protein in complex formation with the H2A histone protein (Suppl. Table S5). The high involvement of multiple hydrophobic amino acids like Phe53, Phe56, Phe33, Leu54, Leu81, Ile88, Leu92, Leu95, Phe84 are direct evidence of the high prevalence of these hydrophobic interactions in stabilization of the protein-protein complex formed between the viral capsid protein and histone protein. The high involvement of Arg55, Arg82, Arg85 and Arg99 also show the predominant role played by the Arginine residue sidechains during heterodimerization between the capsid and histone protein through the involvement of multiple hydrophobic interactions. Similarly, in case of the H2A histone as well, active, dominant and stable involvement of the hydrophobic interactions (Tyr57, Tyr50, Val54, Ala60, Phe25, Glu61, Val30) could be seen through the course of the MD simulation run.

Capsid protein interaction with Histone H2B

Coarse grained *in silico* assembly MD simulation of the C protein and the H2B histone points to the formation of a stable complex between the two as can be ascertained from the RMSD plateau for the last 800 ns of the 1μs MD simulation trajectory with respect to RMSD of protein backbone atoms (Fig. 1B). Clustering analysis of the trajectory points to the formation of one prominent cluster through the course of the coarse grained simulation. Representative structure from this protein complex cluster was simulated using conventional MD simulation in set of three independent replica MD simulations with each extending for 500 ns. Protein backbone atom RMSD analysis of the three conducted simulations point to a stable complex being formed within the initial 50 ns of the trajectories following which RMSD plateau can be seen to be formed (Fig. 4A). Binding energy analysis points to the immense contribution of multiple residues belonging to both the proteins during complex formation. It is observed that most of the major contributing residues of the capsid protein belong to either the hydrophobic pocket or the H4 helix of the capsid protein (Fig. 4B, and Suppl. Table S2). A single residue was found belonging to the N-terminal disordered segment to be participating prominently in the interaction as well. Saturation mutagenesis of these residues point to the importance of multiple residues in the interaction since mutating these residues leads to disastrous consequences on the binding stability of the complex formed between the capsid protein and histone H2B. Mutagenesis studies show that the hydrophobic residues belonging to the hydrophobic pocket are those which are mostly affected owing to mutation. This indicates the importance of hydrophobic interactions during complex formation between the two proteins as has been previously seen as well. The same results are shown by the contact map in (Fig. 4C) where multiple residues belonging to the capsid protein hydrophobic pocket play important role in complex formation between the two proteins. The involvement of majorly the hydrophobic residues of the H2B histone (Phe65, Ile69, Ile73, Tyr37, Ile61, Ile39, Met62, Leu101) are indicative of the same results. Thus it can be hypothesized from these results that the major mode of interaction between the two proteins is due to hydrophobic interactions leading to the burying of the said residues during complex formation in aqueous solution. This leads to increase in the stability of the protein architectures under consideration here. The mode of interaction and



(b)

Residue Mutation	MET37	PHE33	ARG98	MET48	VAL51	ARG9	ARG20	ARG99	LEU95	LEU44	LEU54	TRP47	ARG32
A	2.07	1.14	0.74	2.32	0.88	0.1	0.38	0.12	0.01	0.57	0.47	0.14	0.11
C	1.35	1.01	0.42	1.35	0.85	0.07	0.02	0.09	-0.03	0.41	0.39	0.32	-0.17
D	2.73	1.36	0.64	1.46	1.36	-0.07	0.32	0	0.26	0.38	0.88	0.32	0.33
E	2.5	1.12	0.6	1.29	1.13	0.01	0.57	-0.03	0.09	0.6	0.68	0.28	0.29
F	0.73	0	0.25	1	0.22	0.1	-0.35	0.03	-0.14	0.14	0.01	0	-0.01
G	2.38	1.55	0.62	1.67	1.51	0.32	0.56	0.44	0.27	0.53	0.98	0.58	0.3
H	1.24	0.86	0.26	0.89	0.74	-0.08	-0.04	0.02	-0.08	0.14	0.43	0.32	0.06
I	0.98	0.46	0.32	1.32	0.06	0.03	-0.32	0.02	-0.12	-0.02	0	0.04	-0.13
K	2.49	1.09	0.32	0.89	1.03	0.01	0.52	0.01	0.3	0.53	0.49	0.29	0.21
L	0.75	0.38	0.45	1.14	0.12	0.03	-0.26	0.02	0	0	0	-0.01	-0.08
M	0	0.61	0.39	0	0.36	0.06	-0.19	0.05	0	0.14	0.17	0.12	0.03
N	2.47	1.29	0.44	0.93	1.09	-0.01	0.3	0.08	0.17	0.33	0.72	0.34	0.19
P	1.58	1.35	0.68	1.23	1.02	-0.28	-0.01	-0.1	0.31	0.59	0.98	0.52	0.2
Q	1.98	0.93	0.32	1.13	0.78	0.06	0.51	0.02	0.25	0.41	0.51	0.16	0.1
R	2.16	0.93	0	1.02	0.86	0	0	0	0.18	0.43	0.28	0.07	0
S	2.45	1.22	0.57	1.32	1.24	-0.13	0.27	0.08	0.11	0.46	0.78	0.25	0.22
T	2.03	1.05	0.31	0.91	0.91	-0.1	0.1	0.05	0.03	0.32	0.72	0.23	0.23
V	1.42	0.55	0.27	1.16	0	0.12	-0.22	0.07	-0.15	0.15	0.12	0.07	-0.06
W	0.4	0.07	0.15	0.31	0.3	0.03	-0.29	0.05	-0.01	0.04	0.09	0	-0.04
Y	0.94	0.46	0.17	0.71	0.45	0.1	-0.27	0.04	-0.14	-0.1	0.14	0.06	-0.01

(c)

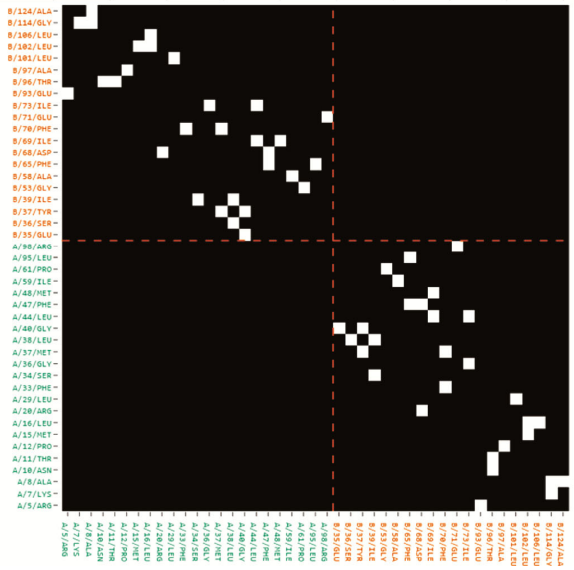
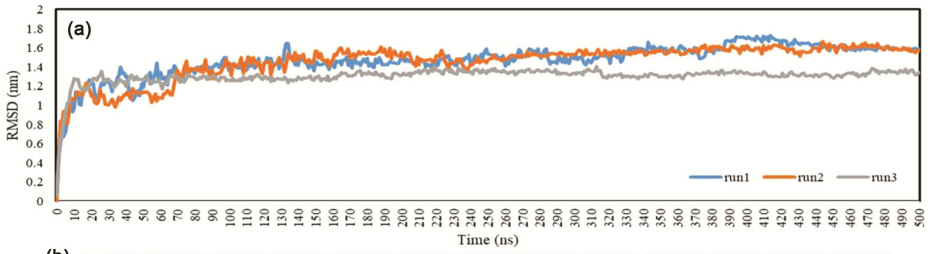


Fig. 4 — MD simulation and post simulation analysis of capsid protein in complex with H2B histone. A. RMSD evolution of the capsid-histone complex backbone atoms through the course of the three 500 ns MD simulation trajectories. B. Saturation mutagenesis analysis of the highest binding energy contributing residues of the capsid protein. C. Inter-chain contact map of Capsid protein in complex with Histone protein

residue involvement during complex formation belonging to the viral capsid protein is similar in this case as compared to the interaction between the C protein and the H2A histone protein i.e. the involvement of the hydrophobic pocket and the H4 helix residues belonging to the capsid protein. An addition in this case is the active involvement of the N-terminal disordered segment and the H1 helix belonging to the capsid protein during complex formation with the H2B histone protein (Suppl. Table S6).

Capsid protein interaction with Histone H3

Conventional MD simulation of the capsid protein in complex with the H3 histone showed the formation of protein backbone RMSD plateau within the first 80 ns of the MD simulation trajectory in case of all the three independent simulation runs conducted for



(b)

Residue Mutation	ARG55	ARG82	ARG22	LEU54	ARG100	ILE78	THR62	PHE56	LEU29	VAL51	LEU92	LYS16
A	1.62	0.66	1.23	2.09	0.48	1.41	0.87	2.81	2.43	2.48	2.22	0.35
C	0.89	0.32	1.19	1.3	0.43	0.99	0.32	2.08	1.86	1.09	1.37	0.12
D	1.02	0.45	1.79	2.29	0.19	1.34	0.89	2.54	2.69	2.24	1.96	0.14
E	1.24	0.43	1.42	1.86	0.18	1.39	1.2	2.65	2.24	2.32	1.68	0.28
F	0.68	0.17	-0.28	0.11	-0.03	0.43	0.05	0	0.81	0.1	0.25	0.03
G	1.13	0.58	2.14	2.52	0.4	1.41	0.9	2.72	2.66	1.91	2.07	0.67
H	0.42	0.11	0.6	0.89	0.04	0.54	0.11	1.81	1.62	1.09	0.77	-0.06
I	0.79	0	-0.09	0.96	0.14	0	0.3	1.08	1.07	0.78	0.95	0.1
K	0.74	0.21	1.04	1.33	0.24	1.51	0.77	2.32	2.1	1.71	0.94	0.12
L	0.62	0.18	-0.07	0	-0.09	0.39	0.23	1.02	0	0.85	0	0
M	0.68	0.15	0.01	0.52	-0.03	0.43	-0.11	1.28	0.81	0.82	0.77	0.31
N	0.64	0.35	1.5	1.69	0.14	1.04	0.52	2.14	2.37	1.63	1.55	0.09
P	1.63	0.91	1.54	1.54	1.09	0.1	0.94	1.67	2.54	1.47	1.92	-0.03
Q	0.89	0.3	1.08	1.56	0.09	1.18	0.47	2.05	2	1.74	0.86	0.2
R	0	0	0	1.08	0	1.25	0.36	1.55	1.56	1.66	0.68	-0.04
S	1.27	0.42	1.49	1.99	0.36	1.2	0.96	2.36	2.6	2.2	1.72	0.23
T	1.2	0.24	0.96	1.46	0.23	0.87	0	2.22	2.08	1.51	1.64	0.01
V	1.12	0.06	0.37	1.32	0.3	0.74	0.54	1.45	1.33	0	1.48	0.3
W	0.66	0.31	-0.44	0.44	0.13	-0.03	0.39	0.53	0.57	0.19	0.04	-0.01
Y	0.7	0.17	-0.28	0.21	0.17	0.22	0	0.9	0.51	0.13	0.3	-0.33

(c)

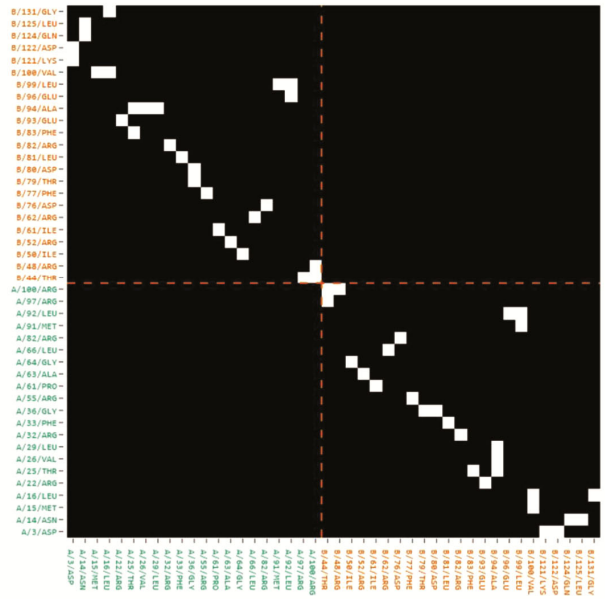
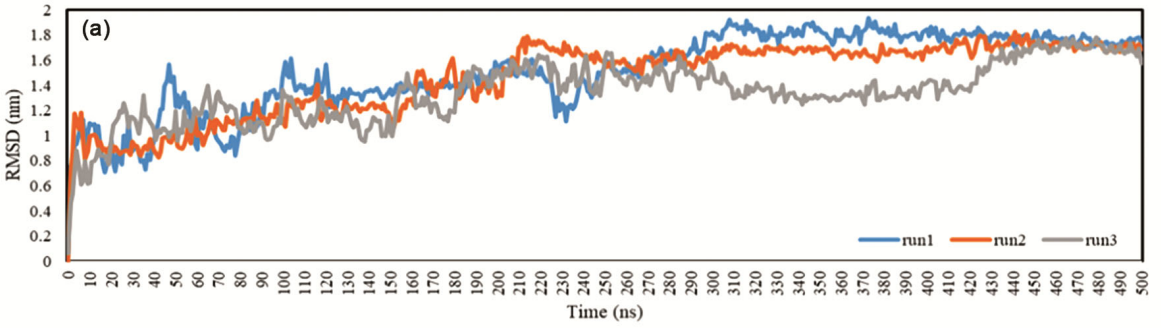


Fig. 5 — MD simulation and post simulation analysis of capsid protein in complex with H3 histone. A. RMSD evolution of the capsid-histone complex backbone atoms through the course of the three 500 ns MD simulation trajectories. B. Saturation mutagenesis analysis of the highest binding energy contributing residues of the capsid protein. C. Inter-chain contact map of Capsid protein in complex with Histone protein

500 ns each (Fig. 5A). This plateau formation is indicative of the highly stable nature of the protein complex formed in this case. Residue wise binding energy analysis and saturation mutagenesis analysis in unison point to the high importance of the hydrophobic pocket and H4 helix belonging to the C protein during its interaction with the H3 histone as is observed through the course of the three MD simulation runs (Fig. 5B, and Suppl. Table 3). Residues like Leu29, Val51, Leu54, Arg55 and Phe56, key components of the capsid protein hydrophobic pocket suffer disastrous consequences with respect to both binding stability of the formed complex as well as binding affinity between the two proteins upon undergoing saturation mutagenesis. Prominent involvement of residues belonging to the



(b)

Residue Mutation	TRP82	LEU46	PHE47
A	0.88	0.53	2.31
C	0.99	-0.01	1.64
D	0.74	-0.05	1.3
E	0.78	0.57	1.6
F	0.18	-0.34	0
G	1.06	0.35	1.78
H	0.26	0.07	0.6
I	0.26	0.07	1.26
K	0.63	0.34	1.25
L	0.23	0	1.26
M	0.22	0.07	0.88
N	0.67	-0.02	0.85
P	0.61	1.4	1.27
Q	0.47	0.23	1.16
R	0	0.1	1.35
S	0.75	0.02	1.51
T	0.66	-0.15	1.56
V	0.25	0.03	1.58
W	0	-0.11	0.62
Y	0.26	-0.25	0.29

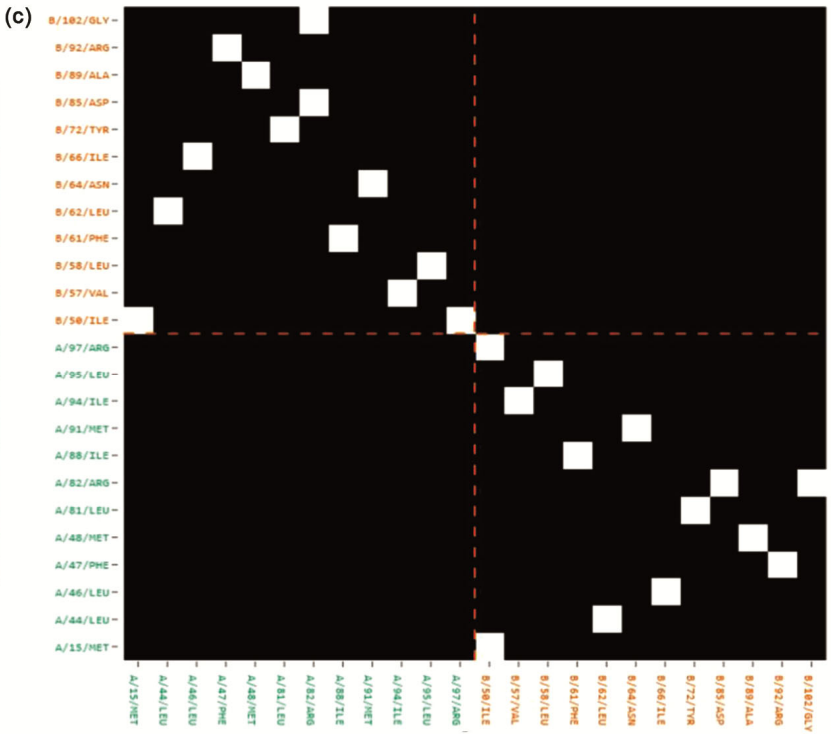


Fig. 6 — MD simulation and post simulation analysis of capsid protein in complex with H4 histone. A. RMSD evolution of the capsid-histone complex backbone atoms through the course of the three 500 ns MD simulation trajectories. B. Saturation mutagenesis analysis of the highest binding energy contributing residues of the capsid protein. C. Inter-chain contact map of Capsid protein in complex with Histone protein

H4 helix of the Dengue virus capsid protein is also observed during complex formation with the H3 histone protein as well indicative of the similar mode of interaction as is observed during formation of the Dengue virus capsid protein dimer[17]. This disastrous effect is evident from the positive values of ΔΔG indicative of decrease in the binding affinity between the capsid protein and the H3 histone. Contact map analysis also point to the extremely high involvement of the hydrophobic amino acids belonging to both the capsid protein and the H3 histone protein (Tyr98, Ile73, Leu102, Phe77, Leu69, Leu99) during complex formation (Fig. 5C). All results point to the crucial role of hydrophobic interactions between the DENV C protein and the histone proteins similar to the previous two cases. The interaction between the viral capsid protein and the H3 histone protein is dominated by the stable interactions involving the four helices belonging to the capsid protein (Suppl. Table S7). Here much more active involvement of the H4 helix belonging to the viral capsid protein can be seen. Similar to the previous interactions, here also active involvement of the hydrophobic interactions is observed.

Capsid protein interaction with Histone H4

Protein backbone RMSD analysis through the course of the triplicate 500 ns MD simulation runs point to the convergence of the MD simulation

systems in the last 200 ns of the MD simulation trajectories (Fig. 6A). Thus, in comparison to the previously studied capsid-histone complexes as mentioned in this study, this capsid protein complex with the H4 histone took an increased time to attain structural stability. Binding energy calculation taking major cluster representatives from all the three MD simulations conducted also point to the less stability of the complex formed between the capsid protein and H4 histone. This lesser binding stability of the Dengue virus capsid protein in complex with the H4 histone is further elucidated by the presence of only three prominent capsid protein residues in the residue wise binding energy contribution analysis (Suppl. Table S4). Saturation mutagenesis analysis of the selected three residues show the high importance of all the three residues with special importance being seen in case of the two aromatic amino acids included i.e. Trp82 and Phe47 (Fig. 6B). Contact analysis shows the involvement of few number of residues belonging to the capsid protein during heterodimer formation with the H4 histone protein (Fig. 6C). These residues could be seen to be constituting the hydrophobic pocket and the H4 helix of the Dengue virus capsid protein indicative of the involvement of this region during dimer formation in this case as well. The lesser number of interacting residues as observed in this case leads to lesser binding stability of the formed complex in comparison to the interaction stability with the other histone proteins under consideration in this study. The same trends have been previously shown during binding energy calculation between the capsid protein and the respective histone proteins. The same thing is observed here as well, where it can be seen that fewer stable and consistent inter-protein interactions are observed when compared to the other three interactions analyzed in this study (Suppl. Table S8). In the few stable interactions observed in this case, majority of the residues involved can be seen to be a part of the capsid protein hydrophobic pocket with lesser active involvement of the H4 helix and almost negligible involvement of the N terminal segment of the capsid protein. As for the histone protein, it can be seen that the central region of the protein shows major involvement in complex formation in this case with important role being played by residues Phe61, Glu53, Leu58, Tyr72, Ile50, Val57, Asp85, Thr54 and Glu74.

Conclusion

Important new information on the molecular interactions between the viral capsid proteins and host cell histone proteins is provided in this study of the Dengue virus capsid-histone complex. Here we have shown that although the DENV C protein interacts with high stability and robustness with all the four core histone proteins, its preference towards the four histones are as follows: H3> H2B> H2A> H4. Through the use of computational techniques, we have elucidated on the complex's structural stability and possible binding mechanisms, identifying important residues making use of *in silico* site directed saturation mutagenesis studies. These residues and the protein-protein interfacial architecture could be used as therapeutic targets. This work opens the door for additional research on stopping the dengue virus's life cycle, ultimately resulting in more potent antiviral treatments.

Acknowledgement

The authors acknowledge CSIR for providing PhD fellowship to Dwaipayan Chaudhuri to conduct this study.

Conflict of interest

Both the authors declare no conflict of interest.

References

1 Lindenbach DR & Rice CM. Flaviviridae: the viruses and their replication. In: Knipe DM, Howley PM, Griffin DE, Lamb RA, Roizman B & Strauss SE, editors. *Fields Virology*, *4th ed. Philadelphia, PA: Lippincott Williams and Wilkins*, (2001). 991.

2 Kuhn RJ, Zhang W, Rossmann MG, Pletnev SV, Corver J, Lenches E, Jones CT, Mukhopadhyay S, Chipman PR, Strauss EG, Baker TS & Strauss JH, Structure of dengue virus: implications for flavivirus organization, maturation, and fusion. *Cell*, 108 (2002) 717.

3 Ng ML, Pedersen JS, Toh BH & Westaway EG, Immunofluorescent sites in vero cells infected with the flavivirus Kunjin. *Arch Virol*, 78 (1983) 177.

4 Bulich R & Aaskov JG, Nuclear localization of dengue 2 virus core protein detected with monoclonal antibodies. *J Gen Virol*, 73 (1992) 2999.

5 Colpitts TM, Barthel S, Wang P & Fikrig E, Dengue virus capsid protein binds core histones and inhibits nucleosome formation in human liver cells. *PLoS One*, 6 (2011) e24365.

6 Marino-Ramirez L, Kann MG, Shoemaker BA & Landsman D, Histone structure and nucleosome stability. *Expert Rev Proteomics I*, 2 (2005) 719.

7 Kiermayr S, Kofler RM, Mandl CW, Messner P & Heinz FX, Isolation of capsid protein dimers from the tick-borne encephalitis flavivirus and *in vitro* assembly of capsid-like particles. *J Virol*, 78 (2004) 8078.

8 Qi Y, Ingólfsson HI, Cheng X, Lee J, Marrink SJ & Im W, CHARMM-GUI Martini Maker for Coarse-Grained Simulations with the Martini Force Field. *J Chem Theory Comput*, 11 (2015) 4486.

9 Van Der Spoel D, Lindahl E, Hess B, Groenhof G, Mark AE & Berendsen HJ, GROMACS: fast, flexible, and free. *J Comput Chem*, 26 (2005) 1701.
10 Bussi G, Donadio D & Parrinello M, Canonical sampling through velocity rescaling. *J Chem Phys*, 126 (2007) 014101.
11 Parrinello M & Rahman A, Polymorphic Transitions in Single Crystals: A New Molecular Dynamics Method. *J Appl Phys*, 52 (1981) 7182.
12 Kubincová A, Riniker S & Hünenberger PH, Reaction-field electrostatics in molecular dynamics simulations: development of a conservative scheme compatible with an atomic cutoff. *Phys Chem Chem Phys*, 22 (2020) 26419.
13 Jo S, Cheng X, Lee J, Kim S, Park SJ, Patel DS, Beaven AH, Lee KI, Rui H, Park S, Lee HS, Roux B, MacKerell AD Jr, Klauda JB, Qi Y & Im W, CHARMM-GUI 10 years for biomolecular modeling and simulation. *J Comput Chem*, 38 (2017) 1114.
14 Essmann U, Perera L, Berkowitz ML, Darden T, Lee H & Pedersen LG, A smooth particle mesh Ewald method. *J Chem Phys*, 103 (1995) 8577.
15 Kumari R & Kumar R, g_mmpbsa - A GROMACS tool for high-throughput MM-PBSA calculations. *J Chem Inf Model*, 54 (2009) 1951.
16 Luger K, Structure and dynamic behavior of nucleosomes. *Curr Opin Genet Dev*, 13 (2003) 127.
17 Byk LA & Gamarnik AV, Properties and Functions of the Dengue Virus Capsid Protein. *Annu Rev Virol*, 3 (2016) 263.